Chapter 5

Experimental Details

The measurements that have been performed are the fusion excitation function spanning the energy range around the barrier and back angle ($\theta_{lab} = 180°$) quasi-elastic scattering excitation function also in the same energy range. As we saw in chapter 2 fusion is defined as the formation of the compound nucleus which decays subsequently. Since the compound nucleus is short lived, only the decay products can be detected to estimate the cross section of the formation of the compound nucleus. The detection of all the decay products like γ-rays, X-rays, charged particles and the final evaporation residue have been used successfully to estimate fusion cross sections. Each technique has its own merits and demerits. In our work we have measured the evaporation residues using a recoil mass separator to estimate the fusion cross section. Measurements of quasi-elastic and elastic cross sections are generally made by detecting the scattered projectile like particles. However, extreme backward angle measurement (near to 180°) are very difficult because of the presence of the beam. These measurements can be performed by detecting the corresponding target like particles going in the forward direction with some device to filter out the beam. We have performed quasi-elastic scattering measurements at a laboratory angle of 180° by detecting the recoiling target like particles after rejecting the beam using the recoil mass separator, HIRA.

The experiments reported in this thesis were performed using the beams provided

by the 15UD, 16 MV Pelletron accelerator at the Nuclear Science Centre (NSC), New Delhi, India. The Pelletron is a tandem Vande Graf accelerator the details of which are discussed in [1, 2]. Pulsed beams were used for all the measurements. This was required for the time of flight measurements which were employed to measure very low cross sections. The recoil mass separator HIRA (Heavy Ion Reaction Analyser) [3] was used in all the measurements the details of which are discussed in the next section.

5.1 The Heavy Ion Reaction Analyser

The Heavy Ion Reaction Analyser (HIRA) is a large solid angle online mass separator for the reaction products preserving their kinematic correlations. It is designed to effectively separate the nuclear reaction products of interest from the elastically scattered beam, dispersing them with good mass resolution at its focal plane with energy and space focusing. This is ideal for studying reactions which are forward peaked and has good application in the study of fusion and transfer reactions around the Coulomb barrier, spectroscopy by residue tagging etc. The HIRA has an energy acceptance of ± 20 % and mass acceptance of $\pm$ 5%. The distance from the target position to the focal plane is $\approx$ 8.5 m and the transport time of ions through HIRA is of the order of a fraction of μs to a few μs depending on the energy of recoils.

The Configuration - The electromagnetic configuration of HIRA is QQ-ED-M-MD-ED-QQ. Here QQ stands for the quadrupole doublet, ED for the electrostatic dipoles, MD for the magnetic dipole and M for the multipoles. The first order performance of the system is given by six parameters: the bending radii and angles of the ED's (ρ_E, θ_E) and the MD (ρ_M, θ_M), the separation (d) between the effective field boundaries of the ED and MD and the angles (α) of the entrance and exit pole faces of the MD. A list of the relevant parameters of HIRA is given in Table 5.1. Further details about the various components can be found in Ref. [3].

One of the specialties of HIRA is the provision for rotation about a fixed axis.

Parameter	Design Value
Quad Q1 Leff	300 mm
Aperture rad. of Q1 and Q2	60 mm
Max. gradient of Q1 and Q2	10 T/m
Quad Q2 Leff	230 mm
ED1 and ED2:	
Bending radius	5 m
Bending angle	16°
Electric rigidity	15 MV/q
Plate separation	150 mm
Magnetic Dipole (MD):	
Bending radius	0.86 m
Bending angle	36° (36.3)°
Magnetic rigidity	48.5 MeV-amu/q^2
Entrance and exit shim angles	7°,(7.2°), 7°,(7.4°)
Radii of curvature of entrance and exit EFBs	2.33 m
Pole gap	80 mm
Pole width	600 mm
Q3-Leff	325 mm
Aperture radius (Q3,Q4)	75 mm
Max. gradient (Q3,Q4)	6.5 T/m
Q4-Leff	430 mm
Multipole (max. fields at x = 100 mm):	
Quadrupole	185 G
Sextupole	90 G
Octupole	60 G
Leff	300 mm
Max. solid angle:	
With $\delta_E = \delta_M = 0\%$	11.3 (10) msr
With $\delta_E = \pm 10\%$ and $\delta_M = \pm 5\%$	9.3 msr

Table 5.1: List of relevant parameters of the Heavy Ion Reaction Analyser (HIRA)

The HIRA can be rotated from angles -15° to +40° maintaining very high vacuum. This is achieved with the help of the sliding seal scattering chamber. Typical vacuum which can be obtained in the chamber is of the order of 10^{-7} Torr. The chamber has an inner diameter of 300 mm and a height of 200 mm and having a movable top lid. The target ladder is mounted through the ports provided in the top lid.

5.2 The Detector Setup

The detector setup consists of detectors used at the focal plane of HIRA and the monitor and other detectors mounted in the scattering chamber.

5.2.1 The Focal Plane Detector System

The recoil mass separator focuses the reaction products at the focal plane after dispersing them according to their m/q values. Thus different m/q groups will be focused at different positions of the focal plane. These reaction products can be identified with the help of detectors which can give both position and energy information. They can either be gas detectors or solid state detectors. For heavy ion detection, gas filled detectors are better suited because of the flexibility in the geometry and also due to less susceptibility to radiation damage. But they have poor energy resolution compared to solid state detectors and the ion detection becomes difficult especially at lower energies. The solid state detectors have the advantage of better energy resolution and can also be used for detection of ions of very low energy. In our experiments we have used a large area position sensitive silicon strip detector.

The Silicon Strip Detector:- The large area silicon strip detector used in the experiments is a 50 mm × 50 mm active area detector supplied by the Micron Semiconductors, England. This detector having the X-1000 design has 16 strips of 3mm width each in the Y-plane and a resistive layer in the X-plane. The detector has a thickness of 1000 microns. Each strip has two outputs, one at each end of the

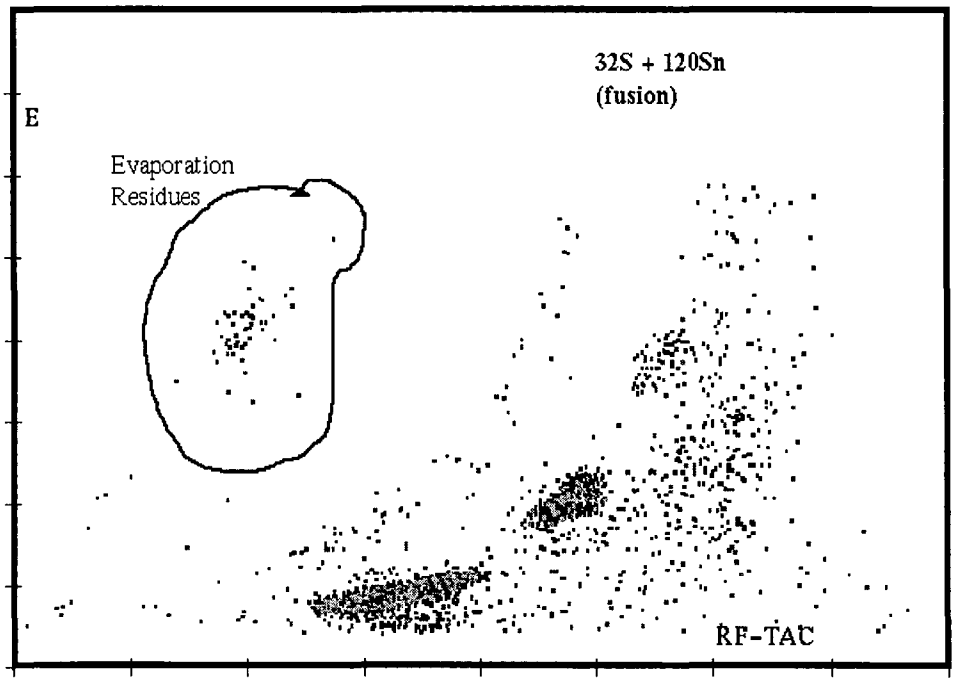

Figure 5.1: A typical two dimensional plot of TOF vs Energy at a very sub-barrier energy. A clear separation of the ER's from the background can be seen.

strip, that makes a total of 32 connectors. Apart from this there is a connector to the back plane which is the cathode and another connector to the PCB ground. The bias is applied to the cathode. A 34 pin ribbon cable connector is used as the interface. The energy signal is obtained from the back plane connector and the position signal is obtained from one end of each of the strips after grounding the other end with a zero ohm terminator. Since in experiments with HIRA we are interested in getting a continuous position, the detector was used in a different configuration. In this case, all the 16 strips were shorted at both the ends thereby making the detector a square wafer of active area 50 mm $\times$ 50 mm. In this configuration the total energy is taken from the back plane and the position information from one of the shorted ends after grounding the other end. The detector was used with positive bias voltage in the range 30 - 60 Volts with leakage currents varying from 0.35 to 0.56

μA. The preamplifier used in the biasing circuit was 142B (ORTEC) with 10 MΩ input impedance.

5.2.2 The Four Monitor Detector Arrangement

Monitor detectors are generally used for beam flux normalisation and beam monitoring. In normal measurements a single or two detectors are used for beam monitoring. But in high precision cross section measurements, there is a need for more accurate beam monitoring in order to lock the beam spot on the target in both x and y direction. To achieve this a set of four monitor detectors was used. All four detectors were kept out of plane of the beam at an angle of 20° thereby giving a reaction angle of 28°. At this angle the scattering is totally Rutherford which is essential for normalisation purposes. The monitor detectors used were silicon surface barrier detectors with 100 micron thickness and 100 mm^2 active area. A collimator of 3 mm diameter was used for the detectors.

5.3 Other Experimental Details

5.3.1 Target

The target used for the experiment were thin foils of enriched Sn isotopes - ^{112}Sn (96.3 % enriched), ^{116}Sn (99 %), ^{120}Sn (98 %). Thin targets were used so as to minimise the energy and angular straggling effects for the recoils and also for the incident beam. The thickness of the targets used was 77 $\mu g/cm^2$, 85 $\mu g/cm^2$ and 50 $\mu g/cm^2$ for the ^{112}Sn, ^{116}Sn, ^{120}Sn targets respectively. All targets were evaporated on carbon backing of $\approx$ 10 $\mu g/cm^2$. The thickness of the targets and carbon backing was measured using the energy loss of 5.486 MeV α-particle through the foil.

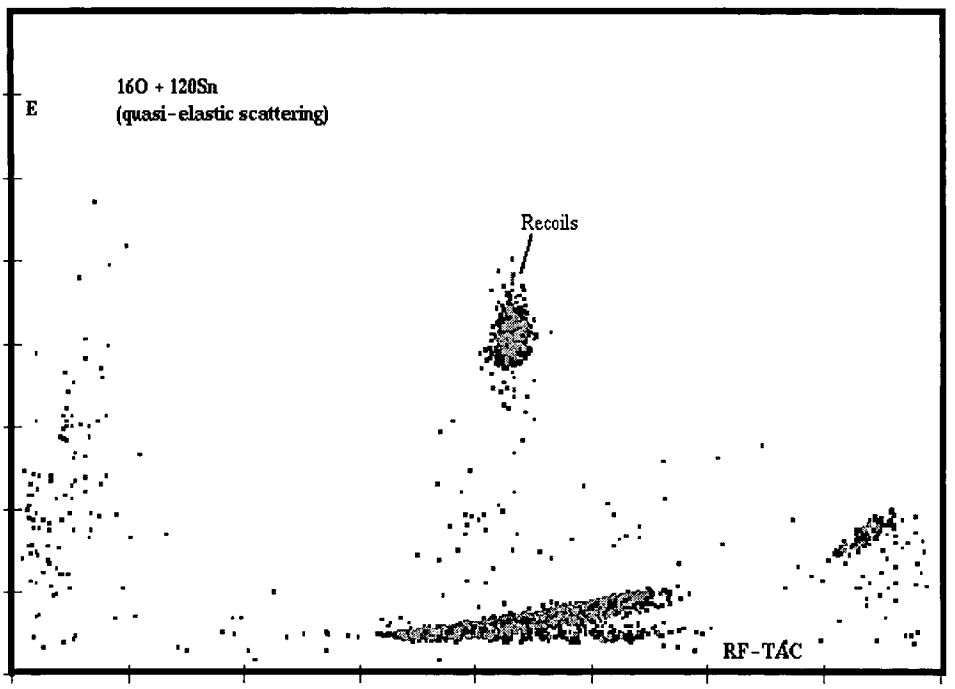

Figure 5.2: A two dimensional plot of TOF vs Energy for the quasi-elastic scattering for ^{16}O + ^{120}Sn. The recoiling target like particles are clearly separated from the the background.

5.3.2 Time of Flight Measurement with Pulsed Beam

In our measurements we have used pulsed beam instead of DC beam. The pulsed beam given by the Pelletron normally has a repetition rate of 250 ns. For our measurements we employed the TWD (Traveling Wave Deflector) to chop off the intermediate pulses to get repetition rates of even multiples of 250 ns. This pulsed beam was used to record the time of flight for the reaction products through HIRA. The length of HIRA is nearly 8.5 m so the flight time of the recoils through HIRA roughly ranges from 1 μs to 4 μs. The repetition rate of the beam was chosen to be more than the flight time of the recoils. In a two dimensional plot of energy *vs* time of flight a clear separation was seen between the evaporation residues and elastically scattered beam. This was effective even in the case when the ER energy

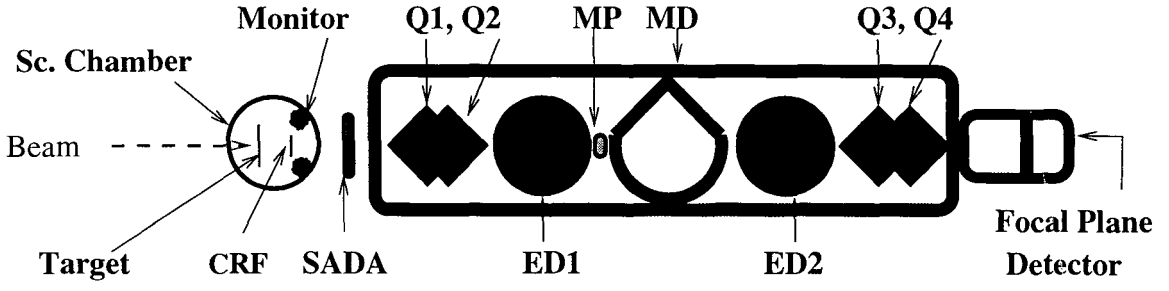

ED1, ED2 - Electric Dipoles ; MD - Magnetic Dipole ;
Q1,Q2,Q3,Q4 - Quadrupoles ; MP - Multipole element ;
SADA- Solid Angle Defining Aperture; CRF- Charge Reset Foil

Figure 5.3: **Schematic of experimental setup.**

was small of the order of 7 - 8 MeV. Since a clean separation could be achieved, measurements up to very low cross sections were possible (Fig. 5.1). We measured upto 100 μbarns of cross sections without any difficulty. This method of suppressing beam background was also useful in the quasi-elastic cross section measurements. The measurement of forward recoiling target like particles at the focal plane of HIRA is very difficult as there will be huge background from the scattered beam. This problem is compounded when the system studied is not very asymmetric as then the beam rejection by HIRA is not very good. Since the scattered beam will not have any fixed time structure they can be easily separated in a two dimensional plot of energy *vs* time of flight. With this technique we could measure quasi-elastic scattering cross sections at 180° which had not been measured earlier (Fig. 5.2).

5.3.3 Experimental Setup

The schematic of the experimental setup is shown in Fig. 5.3. The targets were mounted on a target ladder which has four slots. A quartz crystal was used in one of the slots for viewing the beam spot using a CCD camera and TV monitor. Four silicon surface barrier detectors (SSB) were used in the target chamber for beam

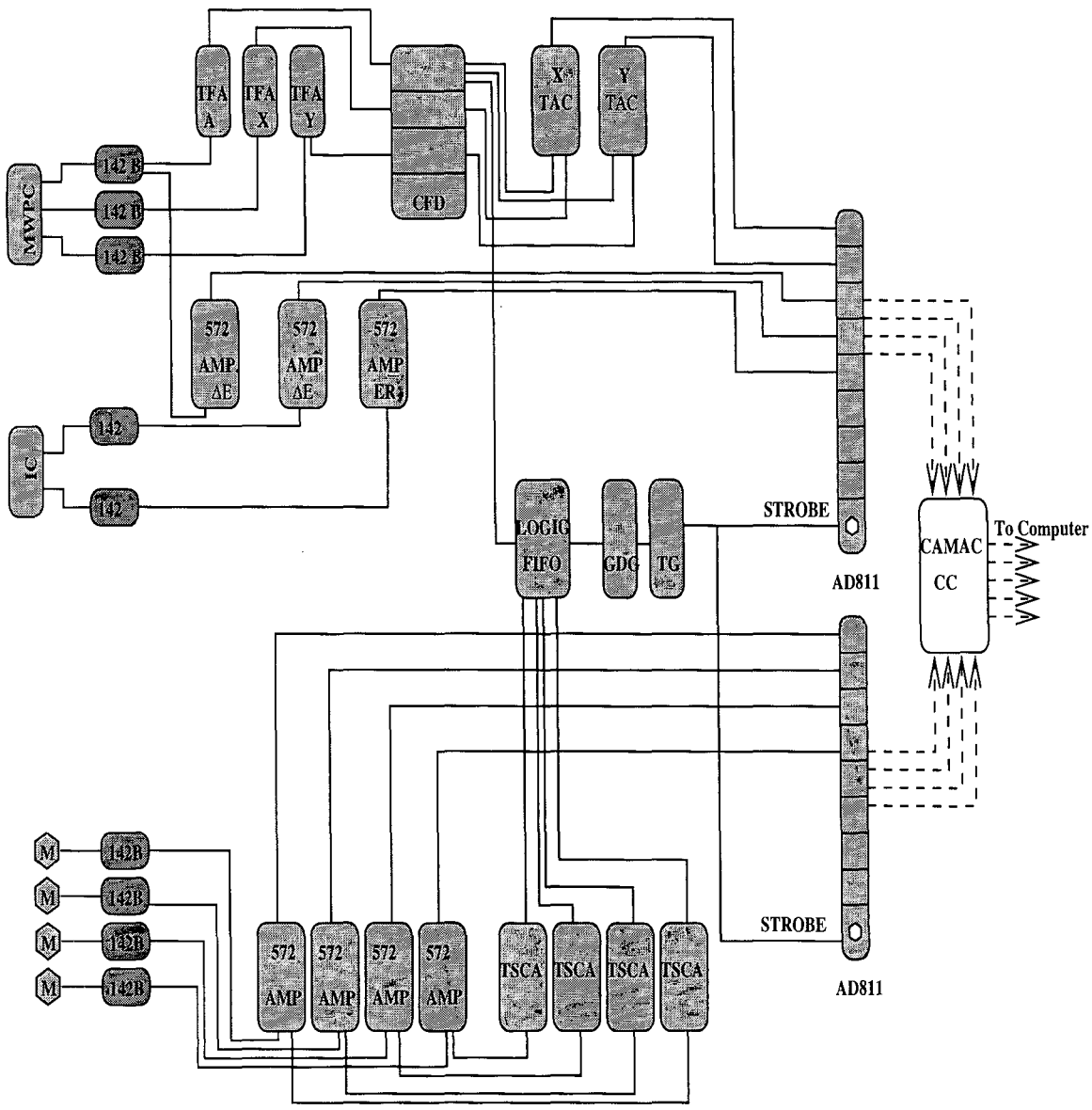

Figure 5.4: **Block diagram of the electronic setup for the experiments.**

monitoring and beam flux normalisation. They were kept at a distance of 11 cm from the target and the solid angle subtended by each monitor detector was 0.785 msr. The focal plane plane detector used was a large area silicon strip detector.

Charge Reset Foil

At a given beam energy the distribution of charge states of evaporation residues is determined by atomic processes which occur within the target and internally converted γ-transitions occurring after the product has recoiled from the target. A thin carbon foil of ≈ 5 μg/cm^2 was inserted at a distance of $\sim$10 cm away from the target in the direction of the residues so that the charge state of the residue shifted due to internal conversion is re-equilibrated.

Optimisation of the RMS

The reaction products were selected by setting the HIRA fields (ED's, MD, Q1, Q2, Q3 and Q4, and the multipole) with the help of the HIRA control system. The fields were optimised to maximise the transportation of the reaction products to the focal plane.

Signal Processing and Data Collection

A schematic of the electronics setup used in the measurements is shown Fig. 5.4. The processed data has been collected online using the data acquisition program FREEDOM [4]. Collected data were stored in compact discs for offline sorting.

5.4 Detection Efficiency

The calculation of absolute cross sections requires that we know the efficiency of the measuring instrument accurately. When making measurements with HIRA the total efficiency of detection consists of the efficiency of the detector used at the focal plane and the transport efficiency of HIRA. The total detection efficiency can be considered as a product of the following four quantities, namely

1. the position dependent efficiency,
2. energy dependent efficiency,
3. charge state fraction,
4. angular distribution dependent efficiency factor

which together defines the transport efficiency of HIRA intrinsically including the efficiency of the detector.

The measurement of the absolute efficiency of HIRA for a particular ion can be made using coincidence of ER's detected at the focal plane with their characteristic gamma rays emitted at the target position. Ratio of the area of the identified coincidence gamma line to that of the singles for a particular residue will give the transport efficiency for the same. This method is simple and gives the efficiency for individual channels, however it cannot be employed effectively for getting estimates of the efficiencies of weak evaporation channels. In the case of weak channels, the intensity of the γ-lines will become very low and their identification becomes quite difficult. Also when using thin targets, as it is in our case a lot of time is required to get sufficient statistics. Alternatively, the absolute detection efficiencies for various evaporation channels at different beam energies can be obtained by a combination of theoretical estimate of energy and angular distributions of residues and experimental determination of these distributions and charge state distribution for certain selected cases [5]. For the theoretical estimate of energy and angular distributions, the Monte Carlo code PACE2 [6] can be used.

1. **Position dependent transport efficiency** - The recoil mass separator is designed to transport the ions to all positions in the focal plane with equal efficiency. However the small deviations in the trajectories of the ions inside the RMS results in the variation of the transport efficiency across the focal plane. The measurement of this relative efficiency as a function of HIRA focal

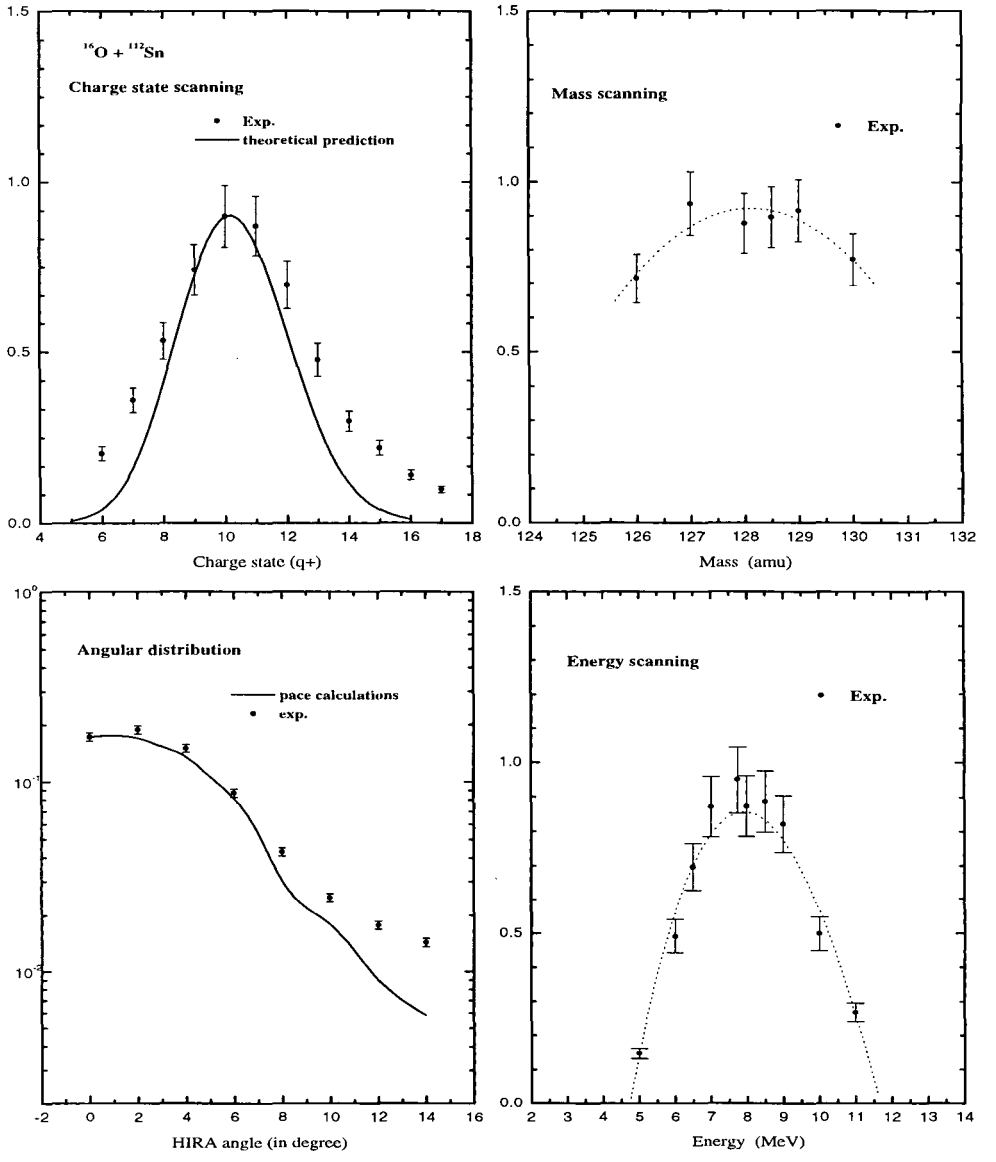

Figure 5.5: Measured charge state, mass, energy and angular distributions for the system $^{16}O + ^{112}Sn$ at a beam energy of 70 MeV.

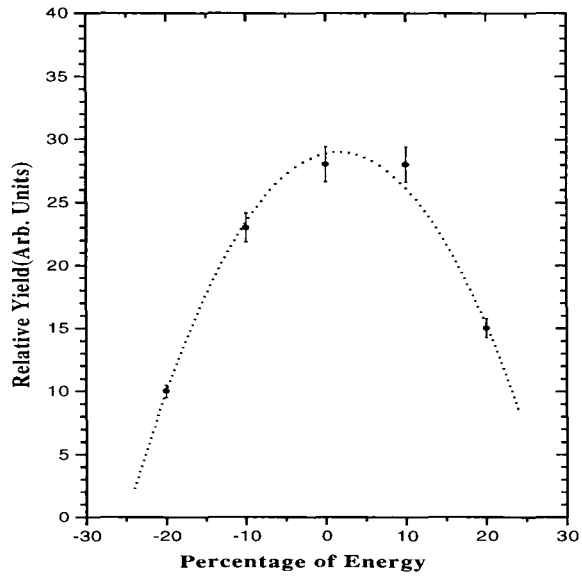

Figure 5.6: Measured energy acceptance of HIRA using α source.

plane position was done by changing the HIRA fields which scans a particular mass peak across the focal plane position. A plot of focal plane yield *vs* the focal plane position is shown in (Fig. 5.5).

2. **Energy dependent transport efficiency** - The energy acceptance of HIRA for the evaporation residue has been measured by setting the HIRA fields for different values of the ER energy. The yield was measured for a particular mass at different set energies and plotted against the set energy. The ideal energy acceptance of the spectrometer (measured using an α source) is shown in Fig. 5.6. The estimated energy acceptance was found to be ± 20 %. The energy acceptance obtained for the case of ER's is shown in Fig. 5.5.

3. **Charge state fraction** - The evaporation residues, after passing through the target and the charge reset foil will have a distribution of charge state according to its energy. In the measurement of residues, it of great importance to select the charge state having the maximum probability. In order to find the charge

state having maximum yield, the HIRA field was set for different charge states and the normalised yield in a particular mass was plotted against the charge state. The optimum charge state selected was used in the measurements. The charge state fraction estimated has been used in the estimation of the absolute efficiency. The charge state distribution depends on the mass (M), charge (Z) and energy (E) of the particle. The distribution obtained from the experiment is the sum of the distributions for different Z-values forming a particular mass. The total charge state distribution is compared with the predictions of Sayers semi-empirical formula [7] in Fig. 5.5. The distribution was found to be in good agreement with the predictions.

4. **Angular distribution** - The angular distribution of the evaporation residue is measured by rotating the recoil mass separator HIRA to various angle with respect to the beam direction. The fusion products are generally confined in a narrow cone around the beam direction. The measured angular distribution using HIRA is shown in Fig. 5.5. The figure shows the distribution for the system ^{16}O + ^{112}Sn compared with the PACE2 angular distribution. In this measurement, the solid angle of acceptance of HIRA was kept at the minimum value of 1 msr. ER yield was measured at angular steps of 0.5 to 1 degree. Angular distribution has been measured at both positive and negative angles to locate the exact zero degree direction of HIRA. It was found that the shape of the angular distribution does not change very drastically with changing beam energy.

5.5 Systems Studied

The details of the measurements performed for the various systems are outlined here. Our effort was to make precise measurements of fusion and quasi-elastic cross sections so that the barrier distribution could be extracted. The barrier distribution is obtained from the second derivative of the product of the fusion cross section

and the centre of mass energy with respect to energy. Since the error in the second derivative is directly proportional to the absolute error in the cross section, lot of care needs to be taken to minimise the errors in the cross section. To achieve this, the data was collected with statistical precision of 1% or more. Care was taken to minimise the other sources of errors also. The main effort was to lock the beam direction through out the run. This was achieved by maintaining the same beam profile and also monitoring the ratios of the counts in the four monitor detectors. The four monitor detector setup described before was extremely useful in this. In all the measurements we started from the highest energy and always changed energy in one direction so as to minimise the possible errors in the definition of the exact energy due to magnet hysteresis. During energy changes, care was taken in setting the field of the switching magnet and analyser magnet. The field was not allowed to over shoot the desired value so that field is changed only in one direction.

5.5.1 $^{16}O + ^{112,116}Sn$ Systems

Fusion cross section measurements were made for the two systems in the energy range 52 MeV to 70 MeV. The Coulomb barrier for the systems $^{16}O + ^{112}Sn$ and $^{16}O + ^{116}Sn$ are 51.74 MeV (E_{lab}=59.14 MeV) and 50.81 MeV (E_{lab}=57.82 MeV) respectively. The detector set up consisted of four monitor detector in the target chamber placed at an angle of 28° and a large area (50 mm × 50 mm) position sensitive silicon surface barrier detector at the focal plane of HIRA. Pulsed ^{16}O beam of repetition rate 4 μsec was used as the flight time of the recoils through HIRA ranged from 2 to 3 μsec for the two systems in the full energy range. The solid angle of HIRA was kept at 5 msr. At 70 MeV measurements were performed to obtain the energy, mass and charge state distributions for the two systems. The angular distribution was also measured for the $^{16}O + ^{112}Sn$ system at this energy. These were used for getting the efficiency for these system. All care was taken to minimise the random errors in the measurement of the excitation function.

5.5.2 $^{16}O + ^{120}Sn$ System

For this system we measured quasi-elastic scattering cross sections at a laboratory angle of 180° in the energy range 48 MeV to 62 MeV. Measurements were made in steps of 1 MeV starting at 48 MeV. Pulsed ^{16}O beam of repetition rate 2 μsec was used. The target was 50 $\mu g/cm^2$ enriched ^{120}Sn with carbon backing of roughly 10 $\mu g/cm^2$. The experimental setup was same as the other measurements. HIRA was kept at zero degree with respect to the beam direction with the solid angle at 5 msr. The total energy and the time of flight was measured. There was a very good separation between the elastic recoils and the scattered beam in the two dimensional plot of energy and time of flight (Fig. 5.2).

5.5.3 $^{37}Cl + ^{116}Sn$ System

For this system fusion cross section were measured at energies around the barrier. The Coulomb barrier for this system is 102.35 MeV (135 MeV in the equivalent beam energy). The measurement was performed in the energy range 130 MeV to 152 MeV which spans from roughly 5 % below barrier to 12 % above barrier. The experimental setup used was as described before. Pulsed ^{37}Cl beam of repetition rate 250 ns was used . For this measurement a 8 $\times$ 47 mm^2 position sensitive detector was used at the focal plane of HIRA.

Fusion cross sections were measured in 1 MeV steps from 152 MeV to 129 MeV. HIRA solid angle was kept at 1 msr for this measurement as the detector at the focal plane was small. The charge state, energy, mass and the angular distribution of the evaporation residues was measured at two energies (136 and 148 MeV). This was done by setting the HIRA electric and magnetic fields for a particular mass, energy and charge state and then changing them to get the different yields at the focal plane. These distribution were later used to estimate the efficiency of HIRA for this system.

5.5.4 $^{32}S + ^{112,116,120}Sn$ Systems

Measurements were carried out for fusion cross sections in the energy range 110 MeV to 140 MeV for the systems $^{32}S + ^{112,116,120}Sn$. The Coulomb barriers for the three systems are 98.64 MeV (E_{lab}=126.82 MeV), 97.93 MeV (E_{lab}=124.95 MeV) and 97.25 MeV (E_{lab}=123.18 MeV). Pulsed ^{32}S beam of repetition rate 2 μsec was used. The targets were the same as used before and the experiment was carried with the same experimental setup. For the $^{32}S + ^{112,120}Sn$ systems measurements were made in steps of 0.75 MeV while for the $^{32}S + ^{116}Sn$ system measurements were made in slightly bigger steps of 1.5 to 3 MeV. As before, the measurements was started at the highest energy where the charge state, mass and energy distributions for the three systems were also measured. The angular distribution was measured for the systems $^{32}S + ^{112,120}Sn$ at laboratory energy of 140 MeV.

Quasi-elastic scattering cross sections were measured for the $^{32}S + ^{120}Sn$ system in the same energy range as for fusion in steps of 1 MeV. The experimental setup was same as before.

Bibliography

[1] G. K. Mehta and A. P. Patro, Nucl. Instrum. & Methods, **A268**, 334 (1988).

[2] D. Kanjilal, S. Chopra, M. M. Narayanan, I. S. Iyer, V. Jha, R. Joshi, S. K. Datta, Nucl. Instrum. & Methods, **A328**, 97 (1993).

[3] A. K. Sinha, N. Madhavan, J. J. Das, P. Sugathan, D. O. Kataria, A. P. Patro, G. K. Mehta, Nucl. Instr. & Meth. **A339**, 543 (1994).

[4] B. P. Ajithkumar, E. T. Subramanium, R. K. Bhowmick, Proceedings of SANAI98, Bombay, February, 1998

[5] A. M. Vinodkumar, Ph.D. Thesis submitted to Calicut University, India, April 1996.

[6] A. Gavron, Phys. Rev. **C21**, 230 (1980).

[7] R. O. Sayer, Revue de physique appliquëe **12**, 1543 (1972).